Photodegradation of clofibric acid in urban, town, and rural waters: important roles of dissolved organic matter composition

Jingting Chen, Hairong Wen, Chunlei Yu, Yuxuan Yin, Yidi Zhang, Hongbin Wang, Ying Huang* and Kan Wang*

School of Civil and Environmental Engineering and Geography Science, Ningbo University, Ningbo, Zhejiang, China

Natural photolysis was the primary pathway for the transformation of pharmaceutical contaminants in surface water, whereas it could be easily influenced by dissolved organic matter (DOM). This study examined the complex effects of DOM on clofibric acid (CA) photodegradation in urban, town, and rural waters. Our results indicated rural water was the most conducive to CA photolysis followed by town water, then urban water. Quenching experiments revealed humic acid (HA) influenced the direct photolysis of CA mainly through two physical ways: internal filtering and active site competition. Reactive oxygen species were identified to be the main reason for CA photodegradation with fulvic acid (FA) or tyrosine (Tyr) involved, including hydroxyl radicals ($OH^\bullet$), singlet oxygen ($^1O_2$), and excited triplet DOM ($^3DOM^*$). We found that hydroxyl radical oxidation, C–O bond breaking, dechlorination, and rechlorination occurred in CA photolysis. Comparative eco-toxicity results showed that the toxicity of products during the CA natural photodegradation process with DOM involved was higher than CA itself, especially in urban waters. This finding emphasized the potential ecological risk of direct CA discharges in natural water and the need to develop risk management strategies that were critical to the health and sustainability of ecosystems.

1 Introduction

Clofibric acid (CA) was a representative of high-risk PPCPs (pharmaceuticals and personal care products), which was an active metabolite of lipid-lowering drugs. It mainly entered natural water through domestic sewage, hospital wastewater, and industrial emissions (Andreozzi et al., 2003). CA existed in water over the long term with relatively low concentrations (ng/L–µg/L) (Li et al., 2012). It had adverse effects on human health and the ecological environment (Nakada et al., 2007; Yang et al., 2017).

The photolysis in natural water was the primary degradation pathway for a multitude of pollutants in surface water bodies. Photolysis had distinct advantages over alternative methods, including eco-friendliness and high efficiency (Yu et al., 2023; Pan et al., 2023).

Researchers reported that photodegradation played an important role in the migration of PPCPs (Cheng et al., 2024). Packer et al. (2003) found that CA underwent direct and indirect degradation under sunlight irradiation. Nevertheless, the photodegradation of CA could be influenced by various factors in natural water, such as pH, inorganic ions, and dissolved organic matter (DOM) (Guo Z. et al., 2023).

DOM in natural water was an important photosensitizer for indirect photolysis (Chen et al., 2009). DOM was a heterogeneous mixture derived from the biological and biochemical residues of animals and plants. DOM was able to generate reactive oxygen species (ROS) (e.g., $OH^{\bullet}$, $^1O_2$, and $^3DOM^*$) under solar irradiation, which impacted the photodegradation behavior of the organic pollutants (Zhang et al., 2014). Furthermore, DOM was characterized by its extensive distribution, complex compositions, and expansive absorption spectrum (Chen et al., 2022). The broad spectrum of DOM was likely to overlap with the absorption wavelengths of a majority of organic pollutants. This led to an internal filtering effect, which restrained the direct photodegradation of pollutants (Shi et al., 2022). Thus it was necessary to explore the significant role of DOM in the photolysis of organic pollutants. However, there was a notable lack of research exploring DOM's impact on the photodegradation of CA in natural water. Cai et al. observed the sources and compositions of DOM in China's Eastern Plain Lake region for a long time by the satellite (Cai et al., 2024). They discovered that the component structure of DOM varied among different area waters. Furthermore, other studies have revealed that the composition and structure of DOM influenced the effect of photolysis in natural water (Li et al., 2020; Awfa et al., 2020). Carena et al. found DOM composition in lake water could be affected by the season and depth of the lake water via modeling, which in turn influenced the photolytic effect of CA (Carena et al., 2024). Shi et al. explored the effect of DOM from different wastewater sources on CA degradation in the UV/H_2O_2 system, finding DOM generally hindered the CA photolysis degradation (Shi et al., 2022). However, the mechanism and eco-toxicity of DOM composition from different region waters on CA natural photolysis process were unclear and needed to be further explored.

In this study, Humic (HA), fulvic acid (FA), and tyrosine (Tyr) were chosen as three representative types of DOM. The natural photolysis process of CA in different water bodies was studied. The degradation kinetics of CA by single and combined DOM compositions were conducted. The mineralization degree in urban, town, and rural waters was assessed by measuring total organic carbon (TOC) removal. The photolysis mechanism was further investigated by ROS analysis and intermediates identification. Then, a potential degradation pathway of CA was proposed.

2 Materials and methods

2.1 Materials

Clofibric acid ($C_{10}H_{11}ClO_3$, >99%), humic acid, fulvic acid, and tyrosine were obtained from Acros Organics. L-histidine and sorbitol were obtained from Sigma-Aldrich. HPLC grade acetonitrile and methanol were supplied by Sinopharm Chemical Reagent Co., Ltd (Shanghai, China). $NaNO_2$, NaCl, NaOH, and H_2SO_4 were analytical grade without further purified. Milli-Q water (Millipore, France, >18.2 MΩ cm) was used for the preparation of all reagents and solvents.

2.2 Experimental procedure

Reactions were performed in 50 mL glass reactors for photochemical reactor and magnetically stirred (300 rpm) in the multi-port magnetic stirring reaction vessel at room temperature (25°C). To better study the photodegradable mechanism, the solution pH was set at 3.0 based on the initial pH of CA. Initially, reactions started by mixing different concentrations of DOM with a solution containing CA, or other chemicals. After the predetermined time, samples were taken for analysis. Methanol (for HPLC) or $NaNO_2$ (for GC-MS and TOC) was used as quenchers. To ensure repeatability, all tests were performed twice and the averages with error bars (±5%) were shown.

2.3 Analytical methods

The Atlantis® T3 Waters column (4.6 mm × 250 mm, 5 μm) of the Waters e2695 with 2489 UV/Vis detector was used to measure the residual CA concentrations at 227 nm. The limit of detection (LOD) was 50 ng/mL. The mobile phase was 0.5% phosphoric acid/methanol (15/85 (v/v)) at a flow rate of 1.0 mL min^{-1}. The sample solution injection volume was 20 μL. TOC analyzer (TOC-VCPH, Shimadzu, Japan) was employed to measure the TOC. GC-MS (Agilent 8860-GC/5977B-MSD, United States) was applied to analyze the intermediates of CA and the detailed operational parameters are provided in Text S1. For the assessment of eco-toxicity, the Ecological Structure Activity Relationships (ECOSAR) program was utilized to predict the acute and chronic toxicity levels of CA and its intermediates.

The pseudo-first-order kinetics via Equation 1 was applied to model the oxidation of CA.

$$C/C_0 = e^{-kt} \tag{1}$$

where C_0 and C represented the residual concentration of CA at 0 min and t min, respectively. k was the rate constant of pseudo-first-order (min^{-1}), and t represented reaction time.

3 Results and discussion

3.1 Effect of single DOM

3.1.1 Effect of HA concentration

The impact of different HA concentrations on CA degradation under simulated sunlight was illustrated in Figure 1A. It showed that the presence of HA inhibited the photodegradation process of CA. As the HA concentration increased from 0 to 15 mg C/L, the degradation efficiency of CA decreased from 94.3% to 50.8% (Supplementary Figure S1A), with the rate constant of CA degradation decreasing from 3.85×10^{-2} to 8.09×10^{-3} min^{-1}
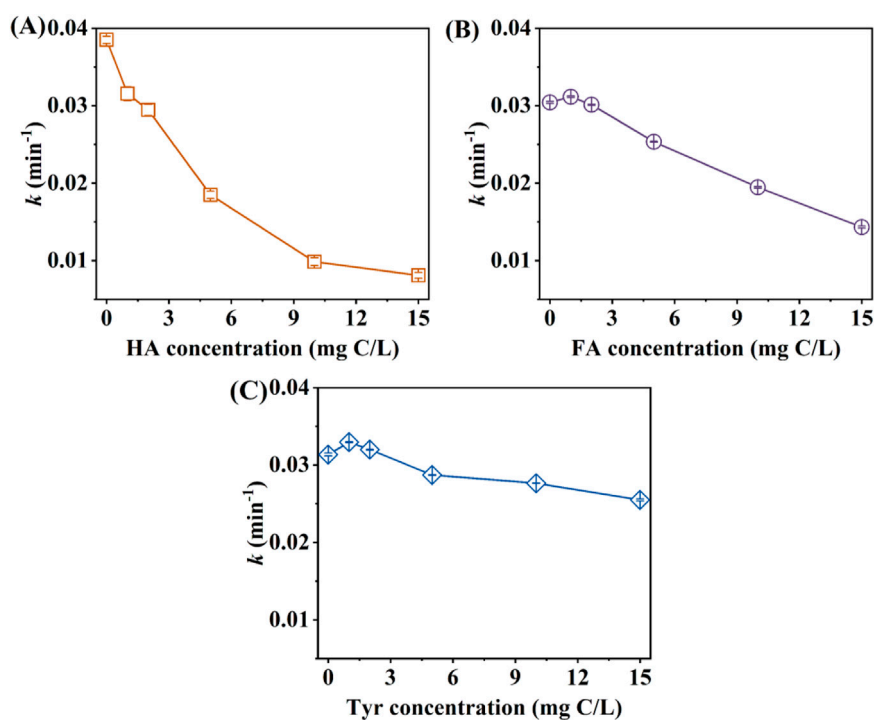
FIGURE 1
Effect of **(A)** HA, **(B)** FA, and **(C)** Tyr concentration on the rate constants k of CA photodegradation. Experimental conditions: $[CA]_0$ = 0.1 mM, pH = 3.0, 500 W xenon lamp.

(Figure 1A). This phenomenon could be attributed to two reasons. On the one hand, HA had a wide ultraviolet absorption band and could compete with organic pollutants in solution for photons (Chen et al., 2022). Due to the overlap of light absorption bands in the xenon emission spectrum, HA and CA could compete for photon absorption. On the other hand, CA was inhibited by internal filtration in the presence of HA (Shi et al., 2022; Guo et al., 2022). Ren et al. reported HA could reduce the contact opportunities between photons and the active sites of target pollutants, leading to an inhibitory effect on CA photocatalysis (Ren et al., 2018). Carlos et al. studied the natural photolysis of the emerging pollutants (EPs) in the presence of humus, including CA, amoxicillin, acetamiprid, acetaminophen, carbamazepine, and caffeine (Carlos et al., 2012). The authors found the increase of substance species in the mixed solution of HA reduced the exposure of photons to the target pollutants (Carlos et al., 2012).

3.1.2 Effect of FA concentration

As shown in Figure 1B and Supplementary Figure S1B, the impact of FA on CA degradation was first promoted and then inhibited, when the FA concentration increased. In the absence of FA, the rate constant k of CA oxidation was 3.04×10^{-2} min^{-1}, while k increased to 3.12×10^{-2} min^{-1} at 1 mg C/L FA (Figure 1B). However, the photodegradation rate decreased significantly with FA concentration further increased. The rate constant of CA degradation reduced from 3.01×10^{-2} to 1.43×10^{-2} min^{-1} as FA concentrations enhanced from 2 to 15 mg C/L (Figure 1B). Keum et al. found the degradation rate constant of PCBs peaked at 150 mg/ L FA concentration (Keum and Li, 2004). At low concentrations of

FA, the direct photolysis of CA might be the primary degradation pathway. Additionally, FA could absorb solar radiation to generate a range of photoactive intermediates, which might facilitate the photolysis of CA (Vaughan and Blough, 1998). Nevertheless, the chemical interaction between CA and high concentrations of FA altered the characteristics and functionality of FA, thereby inhibiting the degradation process of CA (Ren et al., 2019).

3.1.3 Effect of Tyr concentration

The impact of Tyr concentrations on CA photodegradation was investigated. As shown in Supplementary Figure S1C, there was no significant change in CA degradation with different Tyr concentrations. The degradation efficiency of CA was 93.23%, 94.71%, 94.23%, 92.34%, and 91.59%, at 0, 1, 5, 10, and 15 mg C/ L Tyr concentration (Supplementary Figure S1C), corresponding to the rate constant of 3.13×10^{-2}, 3.30×10^{-2}, 3.20×10^{-2}, 2.88×10^{-2}, 2.77×10^{-2}, and 2.55×10^{-2} min^{-1}, respectively (Figure 1C). Compared with HA and FA, Tyr had less effect on CA photodegradation. Bianco et al. discovered that Try exhibited photochemical properties akin to those of HA and FA, whereas Tyr was limited to absorbing sunlight in the ultraviolet-B radiation (UVB) region (Berto et al., 2016). This result limited the photosensitivity of Tyr and reduced its competitive ability with CA for active sites and photons.

3.2 Effect of combined DOM

According to the literature on the composition of DOM in actual water body, we set the DOM concentration at 5 mg C/L in this study
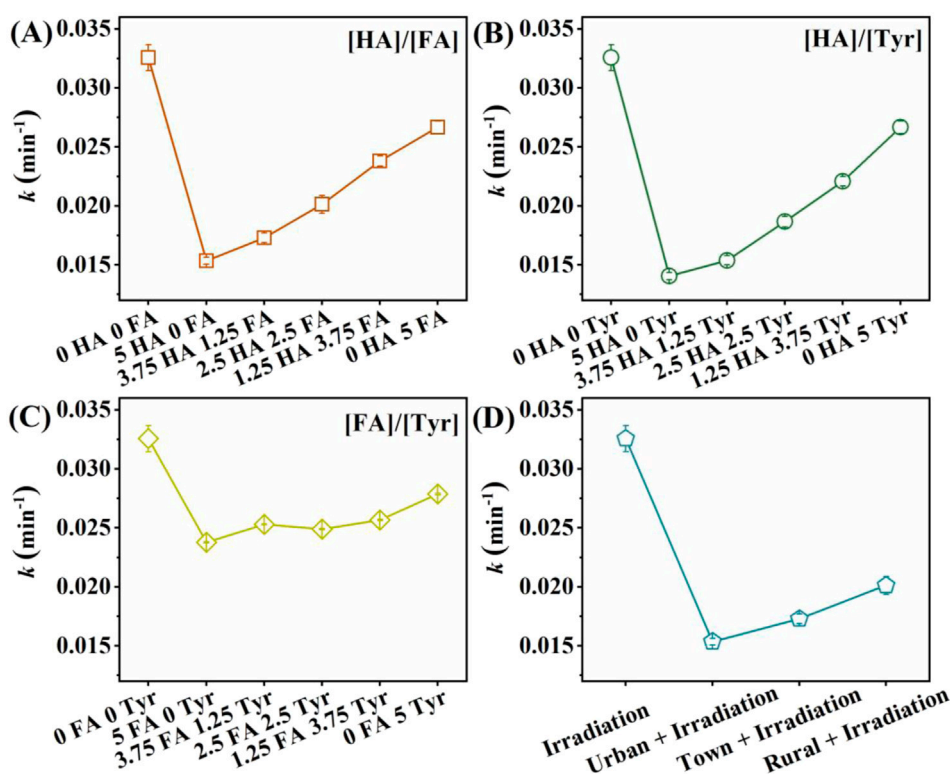
FIGURE 2
Effect of **(A)** [HA]/[FA], **(B)** [HA]/[Try], **(C)** [FA]/[Tyr] and **(D)** different region waters on the rate constants k of CA photodegradation. Experimental conditions: $[CA]_0$ = 0.1 mM, pH = 3.0, 500 W xenon lamp.

(Yu et al., 2018; Xu et al., 2022; Tang et al., 2019; Zeeshan et al., 2024). Xu et al. reported DOM concentrations in town, rural, and urban areas were 3.39 ± 0.60, 3.03 ± 1.26, and 3.02 ± 1.14 mg C/L, respectively (Xu et al., 2022). We explored the mechanism of CA degradation by adjusting the ratios of different DOM compositions. In the absence of combined DOM, the CA degradation rate constant was 3.26×10^{-2} min^{-1}. In general, the photolysis constant of CA decreased with the DOM involved (Figure 2).

As displayed in Figure 2A, the rate constant of CA degradation increased from 1.54×10^{-2} to 2.67×10^{-2} min^{-1} with a reduction in the [HA]/[FA] ratio (Figure 2A). Similarly, when the [HA]/[Tyr] ratio decreased, the CA degradation rate constant enhanced from 1.41×10^{-2} to 2.67×10^{-2} min^{-1} (Figure 2B). These results indicated a significant inhibition of CA photodegradation at high HA concentrations. As shown in Figure 2C, with the [FA]/[Tyr] ratio reduced, the rate constant of CA degradation increased from 2.38×10^{-2} to 2.79×10^{-2} min^{-1}. FA and Tyr had less impact on CA degradation compared to HA, therefore the [FA]/[Tyr] ratio posed a diminished inhibitory effect on CA degradation. The results in single or combined DOM indicated HA was the most effective inhibitor among three types of DOM composition. This could be attributed to the broad absorption spectrum of HA, which interfered with the photolysis process (Chen et al., 2022; Shi et al., 2022).

To observe the photodegradation of CA by DOM in actual water, we simulated the different DOM composition in urban, town, and rural water. Li et al. observed that urbanization levels had a notable impact on the concentration and composition of DOM from four watersheds with different levels of urbanization in Ningbo. Moreover, the DOM concentrations in urban, urban-rural combined, and rural areas were 3.18, 7.45 and 2.16–2.62 mg/L, respectively (Li et al., 2019). Therefore, we set the DOM composition as follows: in urban areas, [HA] = 1.272 mg C/L, [FA] = 0.636 mg C/L, [Tyr] = 1.2084 mg C/L; in towns, [HA] = 1.862 mg C/L, [FA] = 0.894 mg/L, [Tyr] = 4.47 mg C/L; in rural areas, [HA] = 0.84 mg C/L, [FA] = 0.72 mg/L, [Tyr] = 0.84 mg C/L.

As shown in Figure 2D, different regional water bodies exerted different degrees of suppression on the CA photolysis. Among them, the inhibition effect of rural water was the weakest. The rate constant of CA degradation in rural region was 2.01×10^{-2} min^{-1} with 82.83% of CA removal (Figure 2D). It could be attributed to the reason that HA concentration in rural water was lower than that in town and urban water bodies. These findings were consistent with the conclusions drawn from the impact of combined DOM on CA photodegradation (Figures 2A–C). Researchers had suggested that DOM exerted a dualistic influence (promotion or inhibition) on the CA degradation (Janssen et al., 2014). According to previous studies, DOM composition affected its molecular weight, functional group composition, and so on, thereby exerting DOM to exhibit complex and variable properties during photolysis (Wang J. et al., 2019; Janssen et al., 2014). Liu et al. (2023) discovered that DOM from different regions had different group compositions, which influenced the photodegradation of fluoroquinolone antibiotics. In our study, variations in the inhibitory effects of DOM from different regions on CA photolysis also could be attributed to these factors.
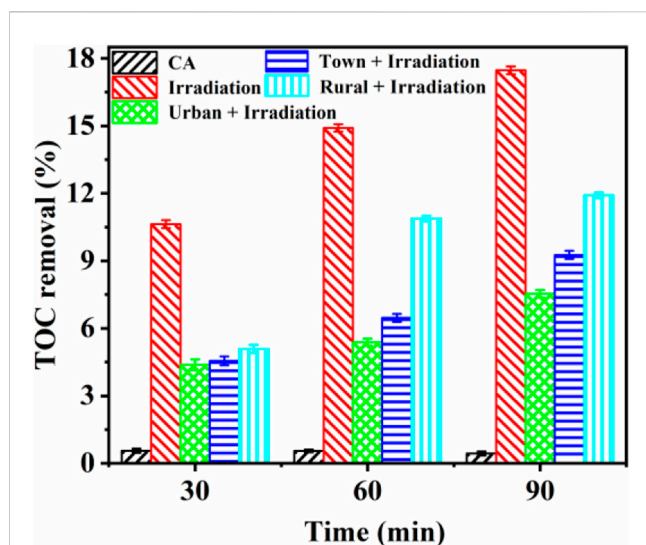
FIGURE 3
TOC removal of CA degradation with different DOM compositions at different reaction times. Experimental conditions: $[CA]_0$ = 0.1 mM, pH = 3.0.500 W xenon lamp.

3.3 Mineralization

However, the rapid degradation did not imply the complete mineralization of CA to CO_2, H_2O, and inorganic salts (Wang Y. et al., 2019). As depicted in Figure 3, CA had almost no mineralization without DOM and solar irradiation. Under irradiation, the mineralization of CA was 10.63%, 14.91%, and 17.47% after 30, 60, and 120 min, respectively. This implied a slight degradation of CA could occur under solar irradiation and the irradiation time might impact the natural photolysis of CA. However, TOC removal of CA in urban, town, and rural regions was reduced to 4.38%, 4.55%, and 5.09% after 30 min solar irradiation, respectively. The high CA photodegradation (Supplementary Figure S2D) but low TOC removal efficiency (Figure 3), might be ascribed to the formation of some refractory intermediates on CA photolysis process (Yuan et al., 2024). With the photolysis time enhanced, CA mineralization in rural water exhibited a significant increase compared to those in urban and town waters. The CA mineralization in rural water achieved 11.92% after 120 min irradiation. The difference in CA mineralization could be attributed to the complex chemical composition and structural characteristics of DOM (Sires et al., 2007). These characteristics
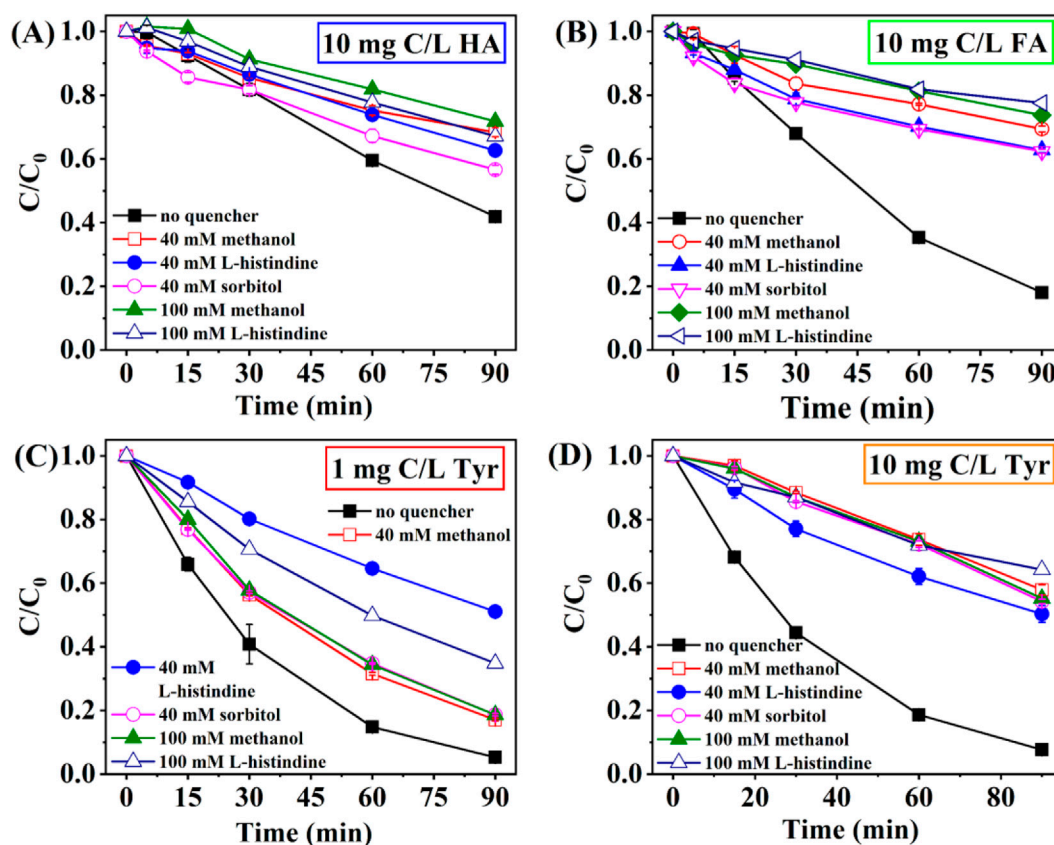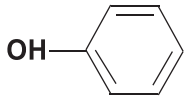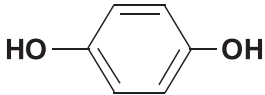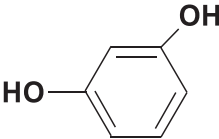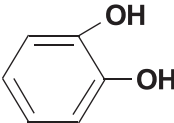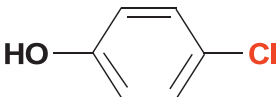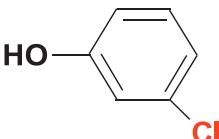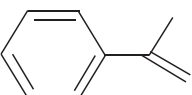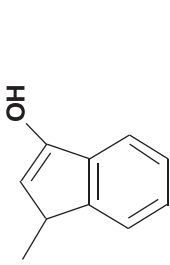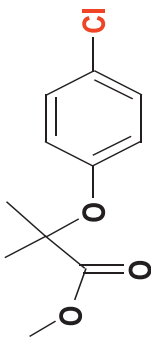

FIGURE 4
Effect of radical scavengers on CA photolysis in the presence of **(A)** 10 mg C/L HA, **(B)** 10 mg C/L FA, **(C)** 1 mg C/L Tyr, **(D)** 10 mg C/L Tyr. Experimental conditions: $[CA]_0$ = 0.1 mM, pH = 3.0, 500 W xenon lamp.

TABLE 1 Major products of CA degradation with different DOM compositions. Experimental conditions: $[CA]_0 = 0.1$ mM, pH = 3.0, 500 W xenon lamp.

NO.	Compound	Proposed structure	Formula	MW (g/mol)	Irradiation	Urban + Irradiation	Town + Irradiation	Rural + Irradiation
P1	Glycerol		$C_3H_8O_3$	92.09	√	√		
P2	Phenol		C_6H_6O	94.11	√	√		
P3	Hydroquinone		$C_6H_6O_2$	110.11	√	√		
P4	Resorcinol		$C_6H_6O_2$	110.11	√			
P5	Catecho		$C_6H_6O_2$	110.11	√			
P6	4-Chlorophenol		C_6H_5ClO	128.00	√			
P7	3-Chlorophenol		C_6H_5ClO	128.00	√	√	√	√
P8	4-Isopropyl phenol		$C_9H_{10}O$	134.07		√	√	√
P9	Diglycolic acid		$C_4H_6O_5$	134.09	√			

TABLE 1 (Continued) Major products of CA degradation with different DOM compositions. Experimental conditions: [CA]$_0$ = 0.1 mM, pH = 3.0, 500 W xenon lamp.

NO.	Compound	Proposed structure	Formula	MW (g/mol)	Irradiation	Urban + Irradiation	Town + Irradiation	Rural + Irradiation
P10	6-Chloro-3-methyl-1-indanol		C$_{10}$H$_{11}$ClO	182.05		✓		
P11	2-(4-chloro phenoxy) -2-methyl propionate methyl ester		C$_{11}$H$_{13}$ClO$_3$	228.06		✓	✓	✓

caused competing interactions and the formation of intermediate products, which collectively contributed to a reduction in the overall extent of mineralization (Li et al., 2009).

3.4 Reactive oxygen species identification

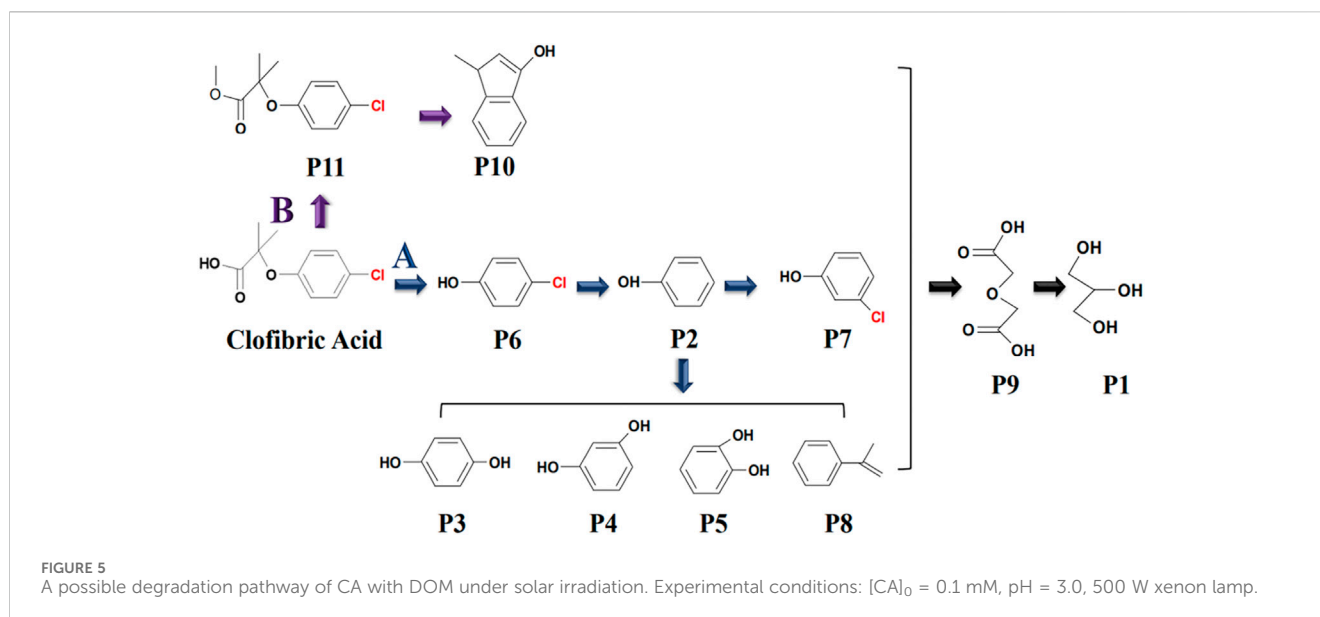In natural water, DOM could absorb sunlight directly due to many chromophores, particularly in the ultraviolet spectrum (280–400 nm). The ground state of DOM could be excited and converted to the triplet state ^{3}DOM*. Furthermore, ^{3}DOM* had the potential to produce reactive oxygen species, which contributed to the indirect photodegradation of target organic pollutants (Jiao et al., 2008; Glover and Rosario-Ortiz, 2013; Leresche et al., 2016; Zeng and Arnold, 2013). Thus, we conducted quenching studies to explore the ROS during CA photodegradation in the presence of single DOM, namely, HA, FA, or Tyr. Methanol, L-histidine, and sorbitol served as scavengers for OH$^\bullet$, ^{1}O$_2$, and ^{3}DOM*, respectively (Gao et al., 2022; Zhu et al., 2019).

As shown in Figure 4A, the photodegradation efficiency of CA was partially inhibited by methanol, L-histidine, and sorbitol presented in the presence of 10 mg C/L HA. Moreover, the quenching effect was not significantly improved with an increase in scavenger concentration. Raising methanol concentration from 40 to 100 mM slightly reduced CA photolysis efficiency from 31.67% to 28.23%. Similarly, CA photodegradation efficiency only reduced from 37.35% to 32.88% by varying L-histidine concentrations from 40 to 100 mM. This phenomenon indicated that OH$^\bullet$ and ^{1}O$_2$ were not the primary ROS at 10 mg C/L HA. CA photolysis efficiency was 43.38% at 40 mM sorbitol. The inhibitory effect of sorbitol was the weakest, indicating the effect of ^{3}DOM* could be negligible. The result further proved that HA might inhibit CA photolysis through photon competition, reducing direct photolysis of CA rather than OH$^\bullet$, ^{1}O$_2$, and ^{3}DOM* being the primary reactive free radicals.

As depicted in Figure 4B, the rate constant of CA degradation achieved 1.95×10^{-2} min^{-1} in the presence of 10 mg C/L FA without radical scavengers. The quenching effect of methanol and L-histidine was obvious. As methanol concentration rose from 40 to 100 mM, the rate constant for CA degradation decreased from 4.11×10^{-3} to 3.22×10^{-3} min^{-1}. Likewise, increasing L-histidine concentration from 40 to 100 mM caused a decline in the rate constant of CA photolysis from 4.96×10^{-3} to 2.85×10^{-3} min^{-1}. Sorbitol could restrain CA photolysis significantly. The photodegradation efficiency of CA decreased from 81.95% to 22.48% with 40 mM sorbitol. These findings highlighted the importance of OH$^\bullet$, ^{1}O$_2$, and ^{3}DOM* in the photodegradation of CA at 10 mg C/L FA. The introduction of scavengers led to a notable decline in CA photolysis efficiency, indicating that FA might affect CA oxidation through indirect photolysis.

Since 1 and 10 mg C/L Tyr had an opposite effect on CA photodegradation, it was necessary to explore the mechanism. In the absence of scavengers, the photolysis efficiency of CA was 94.71% and 92.32% in 1 and 10 mg C/L Tyr solutions, respectively. In Figure 4C, methanol had a slight inhibitory effect on CA photodegradation at 1 mg C/L Tyr, whereas the inhibitory effects significantly enhanced with 10 mg C/L Tyr involved (Figure 4D). This indicated that the formation of OH$^\bullet$ increased with Tyr concentration enhancing. The photolysis efficiency of CA was

FIGURE 5
A possible degradation pathway of CA with DOM under solar irradiation. Experimental conditions: $[CA]_0$ = 0.1 mM, pH = 3.0, 500 W xenon lamp.

81.34% and 45.76% when 40 mM sorbitol was added to 1 and 10 mg C/L Tyr solutions, respectively. This suggested that a considerable quantity of $^3DOM^*$ existed in the 10 mg C/L Tyr solution and participated in the CA photolysis reaction. Therefore, we could speculate that the increase in Tyr concentration was accompanied by an increase in the formation of $OH^\bullet$ and $^3DOM^*$.

When L-histidine concentration varied from 40 to 100 mM, the photodegradation efficiency of CA increased from 48.9% to 65.16% at 1 mg C/L Tyr, but declined from 48.9% to 35.75% at 10 mg C/L Tyr. Excess L-histidine might trigger self-aggregation phenomena, which resulted in a reduced involvement of L-histidine in the reaction (Gao et al., 2022). Therefore, a low concentration of L-histidine (40 mM) exhibited a superior quenching effect. Tyr could only absorb sunlight in the UVB band, which limited its ability to compete for photons, and thus Tyr inhibited CA photolysis mainly through indirect photolysis (Ren et al., 2019). According to the quenching experiments, the inhibitory effect of Tyr on CA indirect photolysis was mainly achieved through the synergistic effect of $OH^\bullet$, $^1O_2$, and $^3DOM^*$.

Due to the diversity of DOM components, the mechanism of different DOM composition on CA photolysis might be in diversity. Based on our findings, HA, FA, and Tyr all exerted their distinct influence on CA photodegradation process. HA predominantly impacted CA photolysis through physical interactions, characterized by photo-filtering and active site competition. Conversely, FA or Tyr inhibited the CA photodegradation mainly via the synergistic impact of various ROS.

3.5 Intermediates identification

To further elucidate the photodegradation mechanism of CA, we employed GC-MS to analyze the products of CA after a 120-min exposure to solar irradiation. Table 1 displayed eleven products identified during CA photodegradation.

The direct photolysis of CA after 120 min of irradiation yielded fewer and simpler products than those found in urban, town, and

rural water. Some typical degradation products of CA was identified and their GC-MS spectra was shown in Supplementary Figure S3, such as phenol (P2), 4-chlorophenol (P6), and 3-chlorophenol (P7) (Zhang et al., 2018; Zhu et al., 2019). The presence of 3-chlorophenol (P7) in the system under irradiation confirmed the existence of dechlorination and subsequent rechlorination reactions during the CA photolytic process. In town and rural waters, the degradation products of CA were the same, namely, 3-chlorophenol (P7), 4-isopropyl phenol (P8), and 2-(4-chloro phenoxy)-2-methyl propionate methyl ester (P11). However, CA intermediates of CA in urban water were more complex than those in town and rural waters. Four additional products were identified, including glycerol (P1), phenol (P2), hydroquinone (P3), and 6-chloro-3-methyl-1-indanol (P10). The intermediates detected were consistent with the results obtained from the photolysis efficiency and mineralization of CA in urban, town, and rural waters. Among three regions, the photolysis efficiency and mineralization degree of CA were the lowest in urban water. This result further confirmed that the composition of DOM in different regions could influence the CA natural photolysis process comprehensively, including removal efficiency, mineralization and intermediates.

3.6 Degradation pathway proposed

Based on the major intermediates of CA and previous studies, a possible photodegradation pathway of CA was proposed in Figure 5. CA photodegradation might be carried out via two pathways in the presence of DOM (Zhu et al., 2019; Zhang et al., 2018).

Pathway A: the cleavage of the C-O bond in CA, resulted in the formation of 4-chlorophenol (P6). Then, P6 dechlorinated to yield phenol (P2). Phenol subsequently underwent a nucleophilic addition reaction, forming a chlorinated aromatic byproduct 3-chlorophenol (P7). Previous research had demonstrated that chlorine atoms on the benzene ring of CA could undergo dechlorination and re-chlorination processes (Zeng and Arnold, 2013). In addition, the ortho, meta, and para position of phenol
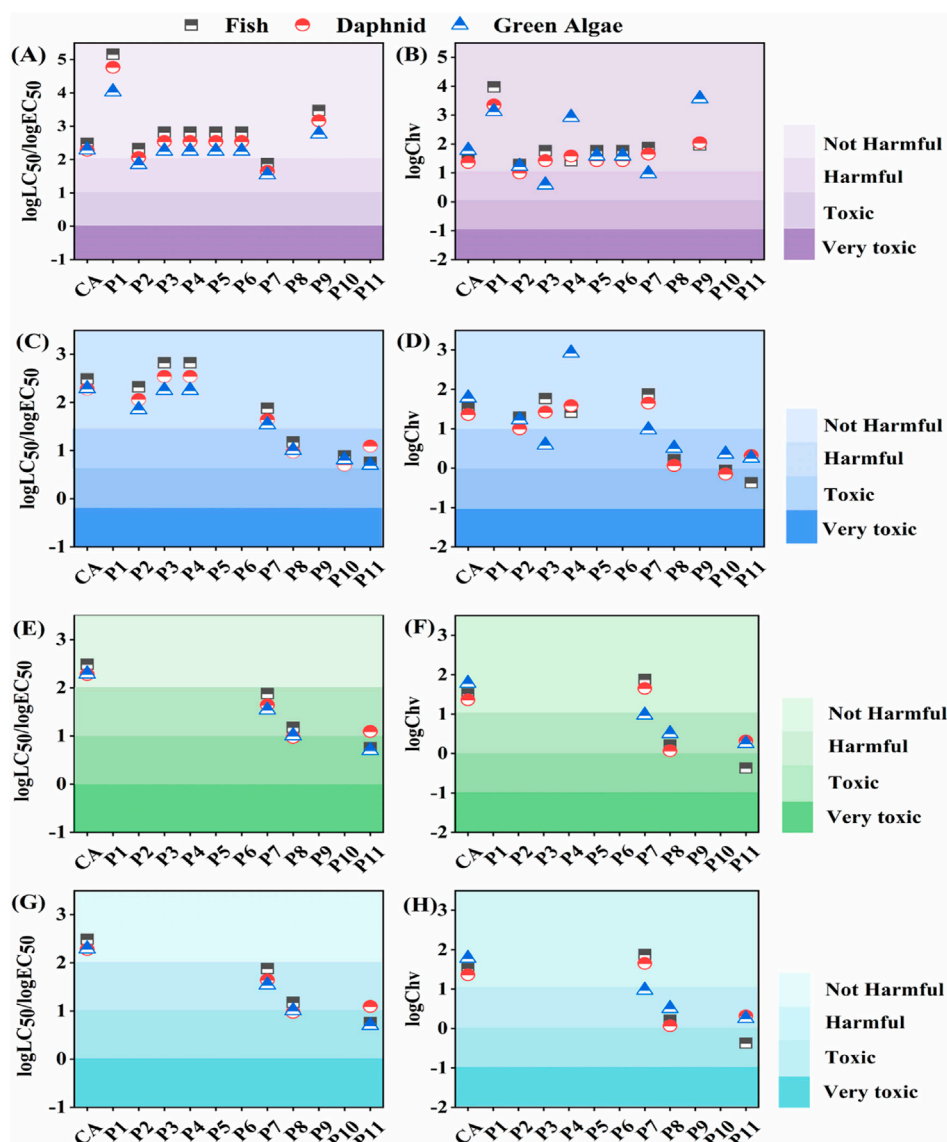
FIGURE 6
Acute toxicity (logLC$_{50}$/logEC$_{50}$) and chronic toxicity (logChv) under **(A, B)** irradiation, **(C, D)** urban + Irradiation, **(E, F)** town + Irradiation, **(G, H)** rural + Irradiation conditions. Experimental conditions: [CA]$_0$ = 0.1 mM, pH = 3.0, 500 W xenon lamp.

became active. Hydroquinone (P3), resorcinol (P4), catechol (P5), and 4-isopropyl phenol (P8) were further formed with ROS involved.

Pathway B: CA could also be reacted to form 2-(4-chlorophenoxy)-2-methylpropionate methyl ester (P11). Then, P11 cyclized to form 6-chloro-3-methyl-1-indanol (P10). Eventually, small molecule products were generated from two pathways, such as diglycolic acid (P9), glycerol (P1), and so on.

3.7 Eco-toxicity assessment

The ECOSAR programs could forecast toxicity metrics, namely, the lethal concentration (LC50), effective concentration (EC50), and chronic toxicity (Chv). Hence, the acute and chronic toxicity of CA and its products to aquatic organisms including fish, daphnia, and

green algae were anticipated by employing the ECOSAR program. The European Union guidelines classify acute toxicity into four groups: very toxic (<1 mg/L), toxic (1–10 mg/L), harmful (10–100 mg/L), and not harmful (>100 mg/L) (Gao et al., 2014). Chronic toxicity levels were assessed according to the Chinese hazard chemical evaluation criteria, categorizing concentrations into very toxic (<0.1 mg/L), toxic (0.1–1 mg/L), harmful (1–10 mg/L), and not harmful (>10 mg/L) (HJ/TI 154–2004; Guo X. et al., 2023). For fish, daphnia, and green algae, CA was at a not harmful level of acute and chronic toxicity.

In Figure 6A, the acute toxicity of CA photolysis with irradiation was based on the values of LC50/EC50. Under irradiation, P2 was harmful to daphnia and green algae, while P7 was at a harmful level to fish, daphnia, and green algae. Other products remained at not harmful levels. In terms of chronic toxicity, P2 (to daphnia), P3 (to green algae), and P7 (to green algae) also reached harmful levels

(Figure 6B). The direct photodegradation of CA without DOM resulted in a minimal increase in ecotoxicity. In urban waters (Figure 6C), acute toxicity of P1, P2, P3, and P7 were at not harmful levels, whereas P8, P10 and P11 increased to harmful levels. Chronic toxicity was more complex (Figure 6D). The toxicity levels of products to fish were aggravated. Chv values of P10 and P11 to fish were 0.884 and 0.425 mg/L, reaching toxic concentrations. In the case of daphnid, P8 and P11 were identified at harmful levels, while P10 exhibited toxic levels. For green algae, a downward trend in Chv values suggested a general increase in toxicity to harmful levels. The eco-toxicity of intermediates in town and rural waters was the same (Figures 6E–H). The acute toxicity of P7 and P8 escalated to harmful levels. Notably, P11 exhibited toxicity to fish and green algae with an LC50 of 5.74 mg/L and EC50 of 4.99 mg/L, respectively. It also posed a harmful level to daphnids, with an EC50 of 12.4 mg/L. As for chronic toxicity, P7 was only harmful to green algae, whereas P8 and P11 were more poisonous to aquatic organisms. The Chv values of P8 (0.068 mg/L) and P11 (0.372 mg/L) achieved toxic levels to daphnids and fish, respectively. The eco-toxicity assessment under different conditions indicated that the natural photodegradation products of CA had a more adverse impact on the ecological environment and merited further attention. This might be due to the more complex structure of intermediates produced during CA photodegradation with DOM involved. It was worth noting that the photodegradation of CA in urban waters presented the highest ecological risk, due to the diversity of products and more toxic to aquatic organisms (e.g., P10 and P11).

4 Conclusion

In this study, we discovered that DOM had a complex effect on CA degradation, owing to its concentration and composition. HA, FA, and Tyr were selected as model DOM in this study. HA demonstrated the most significant inhibitory impact on CA photodegradation. Besides, the photodegradation efficiency, mineralization, and products of CA under natural photolysis conditions in urban, town, and rural waters were further investigated. The results showed that CA photolysis was inhibited in all three water bodies, especially in urban waters. Moreover, CA photodegradation intermediates in urban waters were more abundant and complex. Quenching experiments showed the formation of ROS was correlated with DOM components. HA affected the direct photolysis of CA mainly by filtration and active site competition. The reactions between FA or Tyr with CA were dominated by $OH^{\bullet}$, $^1O_2$, and $^3DOM^*$. GC-MS analysis revealed the presence of some recalcitrant chlorinated organic compounds. The mechanism of CA photolysis included hydroxyl radical oxidation, C-O bond cleavage, dechlorination, re-chlorination, and so on. The degradation pathway of CA in the presence of DOM was further proposed. Eco-toxicological assessment indicated some degradation products might have higher toxicity levels than CA itself in urban, town, and rural waters. Our finding indicated the natural photolysis of pharmaceutical contaminants in natural water may have a detrimental impact on the ecological environment and safe disposal need to be conducted before discharge.

Data availability statement

The original contributions presented in the study are included in the article/Supplementary Material, further inquiries can be directed to the corresponding authors.

Author contributions

JC: Conceptualization, Data curation, Visualization, Writing–original draft. HW: Data curation, Resources, Writing–original draft. CY: Methodology, Resources, Writing–original draft. YY: Resources, Validation, Writing–original draft. YZ: Resources, Validation, Writing–original draft. HW: Data curation, Resources, Writing–original draft. YH: Conceptualization, Funding acquisition, Supervision, Writing–review and editing. KW: Methodology, Supervision, Writing–review and editing.

Conflict of interest

The authors declare that the research was conducted in the absence of any commercial or financial relationships that could be construed as a potential conflict of interest.

Generative AI statement

The author(s) declare that no Generative AI was used in the creation of this manuscript.

Publisher's note

All claims expressed in this article are solely those of the authors and do not necessarily represent those of their affiliated organizations, or those of the publisher, the editors and the reviewers. Any product that may be evaluated in this article, or claim that may be made by its manufacturer, is not guaranteed or endorsed by the publisher.

Supplementary material

The Supplementary Material for this article can be found online at: https://www.frontiersin.org/articles/10.3389/fenvs.2024.1505162/full#supplementary-material

References

Andreozzi, R., Caprio, V., Marotta, R., and Radovnikovic, A. (2003). Ozonation and H$_2$O$_2$/UV treatment of clofibric acid in water: a kinetic investigation. *J. Hazard. Mater.* 103 (3), 233–246. doi:10.1016/j.jhazmat.2003.07.001

Awfa, D., Ateia, M., Fujii, M., and Yoshimura, C. (2020). Photocatalytic degradation of organic micropollutants: inhibition mechanisms by different fractions of natural organic matter. *Water Res.* 174, 115643. doi:10.1016/j.watres.2020.115643

Berto, S., De Laurentiis, E., Tota, T., Chiavazza, E., Daniele, P. G., Minella, M., et al. (2016). Properties of the humic-like material arising from the photo-transformation of L-tyrosine. *Sci. Total Environ.* 545-546, 434–444. doi:10.1016/j.scitotenv.2015.12.047

Cai, X. L., Lei, S. H., Li, Y. M., Li, J. Z., Xu, J., Lyu, H., et al. (2024). Humification levels of dissolved organic matter in the eastern plain lakes of China based on long-term satellite observations. *Water Res.* 250, 120991. doi:10.1016/j.watres.2023.120991

Carena, L., García-Gil, Á., Marugán, J., and Vione, D. (2024). Global modeling of photochemical reactions in lake water: a comparison between triplet sensitization and direct photolysis. *EEH*. doi:10.1016/j.eehl.2024.09.001

Carlos, L., Martire, D. O., Gonzalez, M. C., Gomis, J., Bernabeu, A., Amat, A. M., et al. (2012). Photochemical fate of a mixture of emerging pollutants in the presence of humic substances. *Water Res.* 46 (15), 4732–4740. doi:10.1016/j.watres.2012.06.022

Chen, M., Xu, J., Tang, R., Yuan, S., Min, Y., Xu, Q., et al. (2022). Roles of microplastic-derived dissolved organic matter on the photodegradation of organic micropollutants. *J. Hazard. Mater.* 440, 129784. doi:10.1016/j.jhazmat.2022.129784

Chen, Y., Hu, C., Hu, X., and Qu, J. (2009). Indirect photodegradation of amine drugs in aqueous solution under simulated sunlight. *Environ. Sci. Technol.* 43 (8), 2760–2765. doi:10.1021/es803325j

Cheng, F., Zhang, T., Yang, H., Liu, Y., Qu, J., Zhang, Y. N., et al. (2024). Effects of dissolved organic matter and halogen ions on phototransformation of pharmaceuticals and personal care products in aquatic environments. *J. Hazard. Mater.* 469, 134033. doi:10.1016/j.jhazmat.2024.134033

Gao, L. W., Guo, Y., Zhan, J. H., Yu, G., and Wang, Y. J. (2022). Assessment of the validity of the quenching method for evaluating the role of reactive species in pollutant abatement during the persulfate-based process. *Water Res.* 221, 118730. doi:10.1016/j.watres.2022.118730

Gao, Y., Ji, Y., Li, G., and An, T. (2014). Mechanism, kinetics and toxicity assessment of OH-initiated transformation of triclosan in aquatic environments. *Water Res.* 49, 360–370. doi:10.1016/j.watres.2013.10.027

Glover, C. M., and Rosario-Ortiz, F. L. (2013). Impact of halides on the photoproduction of reactive intermediates from organic matter. *Environ. Sci. Technol.* 47 (24), 13949–13956. doi:10.1021/es4026886

Guo, X., Zhang, H., Yao, Y. Y., Xiao, C. M., Yan, X., Chen, K., et al. (2023a). Derivatives of two-dimensional MXene-MOFs heterostructure for boosting peroxymonosulfate activation: enhanced performance and synergistic mechanism. *Appl. Catal. B* 323, 122136. doi:10.1016/j.apcatb.2022.122136

Guo, Y., Guo, Z., Wang, J., Ye, Z., Zhang, L., and Niu, J. (2022). Photodegradation of three antidepressants in natural waters: important roles of dissolved organic matter and nitrate. *Sci. Total Environ.* 802, 149825. doi:10.1016/j.scitotenv.2021.149825

Guo, Z., Kodikara, D., Albi, L. S., Hatano, Y., Chen, G., Yoshimura, C., et al. (2023b). Photodegradation of organic micropollutants in aquatic environment: importance, factors and processes. *Water Res.* 231, 118236. doi:10.1016/j.watres.2022.118236

Janssen, E. M. L., Erickson, P. R., and McNeill, K. (2014). Dual roles of dissolved organic matter as sensitizer and quencher in the photooxidation of tryptophan. *Environ. Sci. Technol.* 48 (9), 4916–4924. doi:10.1021/es500535a

Jiao, S., Zheng, S., Yin, D., Wang, L., and Chen, L. (2008). Aqueous photolysis of tetracycline and toxicity of photolytic products to luminescent bacteria. *Chemosphere* 73 (3), 377–382. doi:10.1016/j.chemosphere.2008.05.042

Keum, Y. S., and Li, Q. X. (2004). Copper dissociation as a mechanism of fungal laccase denaturation by humic acid. *Appl. Microbiol. Biotechnol.* 64 (4), 588–592. doi:10.1007/s00253-003-1460-y

Leresche, F., Gunten, U. v., and Canonica, S. (2016). Probing the Photosensitizing and inhibitory effects of dissolved organic matter by using N,N-dimethyl-4-cyanoaniline (DMABN). *Environ. Sci. Technol.* 50 (20), 10997–11007. doi:10.1021/acs.est.6b02868

Li, J., Zhang, X., Fan, W. Y., Yao, M. C., and Sheng, G. P. (2020). Dissolved organic matter dominating the photodegradation of free DNA bases in aquatic environments. *Water Res.* 179, 115885. doi:10.1016/j.watres.2020.115885

Li, W., Lu, S., Chen, N., Gu, X., Qiu, Z., Fan, J., et al. (2009). Photo-degradation of clofibric acid by ultraviolet light irradiation at 185 nm. *Water Sci. Technol.* 60 (11), 2983–2989. doi:10.2166/wst.2009.690

Li, W., Shi, Y., Gao, L., Liu, J., and Cai, Y. (2012). Occurrence of antibiotics in water, sediments, aquatic plants, and animals from Baiyangdian Lake in North China. *Chemosphere* 89 (11), 1307–1315. doi:10.1016/j.chemosphere.2012.05.079

Li, Y., Wei, H. J., Wang, K., Zhang, Z. Z., and Yu, X. B. (2019). Analysis of the relationship between dissolved organic matter (DOM) and watershed land-use based on three-dimensional fluorescence-parallel factor (EEM-PARAFAC) analysis. *Huan Jing Ke Xue* 40 (4), 1751–1759. doi:10.13227/j.hjkx.201808118

Liu, S., Cui, Z., Ding, D., Bai, Y., Chen, J., Cui, H., et al. (2023). Effect of the molecular weight of DOM on the indirect photodegradation of fluoroquinolone antibiotics. *J. Environ. Manage.* 348, 119192. doi:10.1016/j.jenvman.2023.119192

Nakada, N., Komori, K., Suzuki, Y., Konishi, C., Houwa, I., and Tanaka, H. (2007). Occurrence of 70 pharmaceutical and personal care products in Tone River basin in Japan. *Water Sci. Technol.* 56 (12), 133–140. doi:10.2166/wst.2007.801

Packer, J. L., Werner, J. J., Latch, D. E., McNeill, K., and Arnold, W. A. (2003). Photochemical fate of pharmaceuticals in the environment: naproxen, diclofenac, clofibric acid, and ibuprofen. *Aquat. Sci.* 65 (4), 342–351. doi:10.1007/s00027-003-0671-8

Pan, T., Tang, Y., Liao, Y., Chen, J., Li, Y., Wang, J., et al. (2023). BiVO$_4$ modifying with cobalt-phosphate cluster cocatalyst for persulfate assisted photoelectrocatalytic degradation of tetracycline. *Mol. Catal.* 549, 113527. doi:10.1016/j.mcat.2023.113527

Ren, D., Chen, F., Ren, Z., and Wang, Y. (2019). Different response of 17α-ethinylestradiol photodegradation induced by aquatic humic and fulvic acids to typical water matrixes. *Process Saf. Environ. Prot.* 121, 367–373. doi:10.1016/j.psep.2018.11.018

Ren, M., Drosos, M., and Frimmel, F. H. (2018). Inhibitory effect of NOM in photocatalysis process: explanation and resolution. *Chem. Eng. J.* 334, 968–975. doi:10.1016/j.cej.2017.10.099

Shi, Y., Geng, J., Li, X., Qian, Y., Li, H., Wang, L., et al. (2022). Effects of DOM characteristics from real wastewater on the degradation of pharmaceutically active compounds by the UV/H$_2$O$_2$ process. *J. Environ. Sci.* 116, 220–228. doi:10.1016/j.jes.2021.12.017

Sires, I., Arias, C., Cabot, P. L., Centellas, F., Garrido, J. A., Rodriguez, R. M., et al. (2007). Degradation of clofibric acid in acidic aqueous medium by electro-Fenton and photoelectro-Fenton. *Chemosphere* 66 (9), 1660–1669. doi:10.1016/j.chemosphere.2006.07.039

Tang, J., Li, X., Cao, C., Lin, M., Qiu, Q., Xu, Y., et al. (2019). Compositional variety of dissolved organic matter and its correlation with water quality in peri-urban and urban river watersheds. *Ecol. Indic.* 104, 459–469. doi:10.1016/j.ecolind.2019.05.025

Vaughan, P. P., and Blough, N. V. (1998). Photochemical Formation of hydroxyl radical by constituents of natural waters. *Environ. Sci. Technol.* 32 (19), 2947–2953. doi:10.1021/es9710417

Wang, J., Chen, J., Qiao, X., Zhang, Y. N., Uddin, M., and Guo, Z. (2019a). Disparate effects of DOM extracted from coastal seawaters and freshwaters on photodegradation of 2,4-Dihydroxybenzophenone. *Water Res.* 151, 280–287. doi:10.1016/j.watres.2018.12.045

Wang, Y., Li, H., Yi, P., and Zhang, H. (2019b). Degradation of clofibric acid by UV, O$_3$ and UV/O$_3$ processes: performance comparison and degradation pathways. *J. Hazard. Mater.* 379, 120771. doi:10.1016/j.jhazmat.2019.120771

Xu, W. N., Yu, H. B., Yang, F., Yang, F., Liu, D. P., Lu, K. T., et al. (2022). Second derivative UV-visible spectroscopy characterizing structural components of dissolved and particulate organic matter in an urbanized river. *Environ. Sci. Eur.* 34 (1), 29. doi:10.1186/s12302-022-00609-z

Yang, Y., Ok, Y. S., Kim, K. H., Kwon, E. E., and Tsang, Y. F. (2017). Occurrences and removal of pharmaceuticals and personal care products (PPCPs) in drinking water and water/sewage treatment plants: a review. *Sci. Total Environ.* 596-597, 303–320. doi:10.1016/j.scitotenv.2017.04.102

Yu, M., He, X., Liu, J., Wang, Y., Xi, B., Li, D., et al. (2018). Characterization of isolated fractions of dissolved organic matter derived from municipal solid waste compost. *Sci. Total Environ.* 635, 275–283. doi:10.1016/j.scitotenv.2018.04.140

Yu, M., Tang, Y., Liao, Y., He, W., Lu, X.-x., and Li, X. (2023). Defect-designed Mo-doped BiVO$_4$ photoanode for efficient photoelectrochemical degradation of phenol. *J. Mater. Sci. Technol.* 165, 225–234. doi:10.1016/j.jmst.2023.06.002

Yuan, Y., Zhang, J., Yin, W., Zhang, L., Li, L., Chen, T., et al. (2024). *In situ* coupling of reduction and oxidation processes with alternating current-driven bioelectrodes for efficient mineralization of refractory pollutants. *Engineering*. doi:10.1016/j.eng.2024.05.009

Zeeshan, M., Ali, O., Tabraiz, S., and Ruhl, A. S. (2024). Seasonal variations in dissolved organic matter concentration and composition in an outdoor system for bank filtration simulation. *J. Environ. Sci.* 135, 252–261. doi:10.1016/j.jes.2023.01.006

Zeng, T., and Arnold, W. A. (2013). Pesticide photolysis in prairie potholes: probing photosensitized processes. *Environ. Sci. Technol.* 47 (13), 6735–6745. doi:10.1021/es3030808

Zhang, D., Yan, S., and Song, W. (2014). Photochemically induced formation of reactive oxygen species (ROS) from effluent organic matter. *Environ. Sci. Technol.* 48 (21), 12645–12653. doi:10.1021/es5028663

Zhang, X., Liu, Z., Kong, Q., Liu, G., Lv, W., Li, F., et al. (2018). Aquatic photodegradation of clofibric acid under simulated sunlight irradiation: kinetics and mechanism analysis. *RSC Adv.* 8 (49), 27796–27804. doi:10.1039/c8ra03140a

Zhu, K., Wang, X., Geng, M., Chen, D., Lin, H., and Zhang, H. (2019). Catalytic oxidation of clofibric acid by peroxydisulfate activated with wood-based biochar: effect of biochar pyrolysis temperature, performance and mechanism. *Chem. Eng. J.* 374, 1253–1263. doi:10.1016/j.cej.2019.06.006